Differential cross sections and spin density matrix elements for $\gamma p \rightarrow \phi p$ from CLAS

Biplab Dey

Carnegie Mellon University

Dec 7th, 2010

Baryons 2010, Osaka

Carnegie Mellon

Jefferson Lab

Outline

1. Introduction and Event Selection
2. Signal-background separation
3. Acceptance Calculation and $d\sigma/d\cos\theta^{\phi}_{c.m.}$
4. Spin Density Matrix Elements
5. Summary

Outline

1. Introduction and Event Selection
2. Signal-background separation
3. Acceptance Calculation and $d\sigma/d\cos\theta^{\phi}_{c.m.}$
4. Spin Density Matrix Elements
5. Summary

Introduction – $\phi(1020)$

- Belongs to the family of ground state vector mesons $V = \rho, \omega, \phi$.
- Almost pure $s\bar{s}$ state – OZI rule suppresses quark/meson exchanges during interaction with nucleons.
- Chief attraction – very "clean" system to study gluonic exchanges; gluonic structure of the Pomeron, for example.
- Around $\sqrt{s} \approx 2.1$ GeV, previous world data (LEPS, SAPHIR) saw a "bump" at $t \longrightarrow |t|_{min}$ (forward-angle). *Not* expected from Pomeron exchange – interference with $K^+\Lambda(1520)$? Resonance contribution?

Charged- and neutral-mode topologies

- ϕ predominantly decays to two kaons. $\phi \rightarrow K^+K^-$ is the "charged-mode" ($bf = 0.491$) while $\phi \rightarrow K^0_S K^0_L$ is the "neutral-mode" ($bf = 0.34$).
- Charged-mode: kinematic fit to $\gamma p \rightarrow \phi p \rightarrow K^+(K^-)p$.
- Neutral-mode: kinematic fit to $\gamma p \rightarrow \phi p \rightarrow K^0_S(K^0_L)p \rightarrow \pi^+\pi^-(K^0_L)p$
- Event selection: 10% confidence level cut from kinematic fit, timing cuts for particle-identification.
- K^0_S selection cut (neutral-mode): $0.488\ \text{GeV} \leq M(\pi^+, \pi^-) \leq 0.508\ \text{GeV}$.

Charged-mode and ϕp-$K^+\Lambda(1520)$ overlap

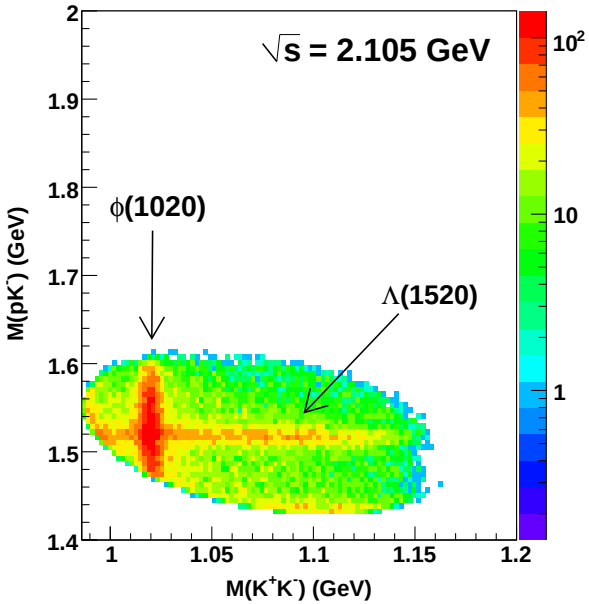

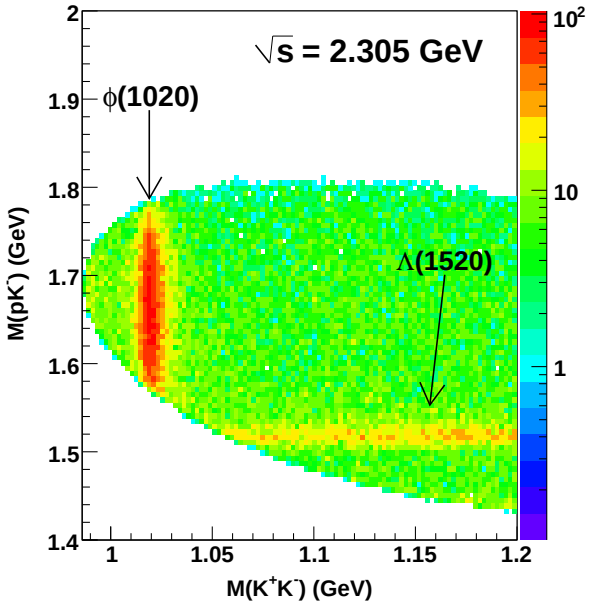

- Overlap with $\gamma p \to K^+\Lambda(1520) \to K^+K^-p$ between 2 and 2.2 GeV.
- Only for the charged-mode, therefore, need for the neutral-mode.

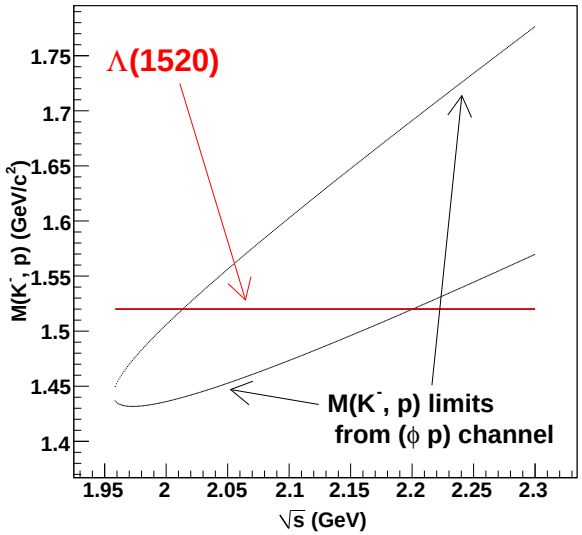

Outline

1. Introduction and Event Selection
2. Signal-background separation
3. Acceptance Calculation and $d\sigma/d\cos\theta^{\phi}_{c.m.}$
4. Spin Density Matrix Elements
5. Summary

General set-up

- Since the ϕ mass is so close to the KK threshold, very few events on the low mass side. Therefore, side-band subtraction is difficult to perform.
- Previous analyses often used background "template shapes" ($\Lambda(1520)$, $f_0(980)$, KK phase-space, etc.), but the scales of these "templates" were not constrained by any physics.
- Our method:-
  - Use the mass-dependent Breit-Wigner width for the ϕ lineshape in the Voigtian signal function.
  - Background level shape/scale depends on location in phase-space, therefore perform individual background fits in localized regions of phase space.
  - Final output is a quality-factor (Q-value) for each event – probability of the event being a good signal (ref: arXiv:0809.2548). Much better/easier control over systematics.

Charged-mode: $K^+\Lambda(1520)$ cut

- After all cuts and background removal, a $M(p, K^-) = 1.52$ GeV "band" still visible, especially in mid-angles. Shown for 2.08 GeV $\leq \sqrt{s} \leq$ 2.12 GeV below:

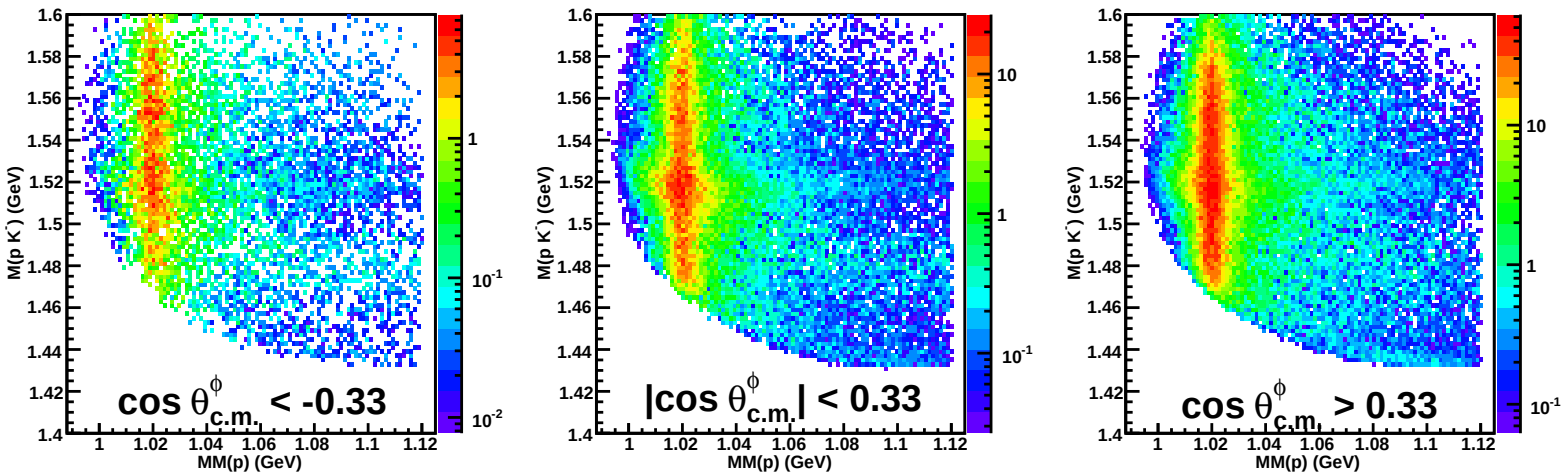

- ϕp and $K^+\Lambda(1520)$ seems to be somewhat strongly correlated in phase-space.

- Apply $|M(p, K^-) - 1.52 \text{ GeV}| \leq 15$ MeV cut for $\Lambda(1520)$ removal

Charged-mode: final results

- $\sqrt{s} = 2.095$ GeV

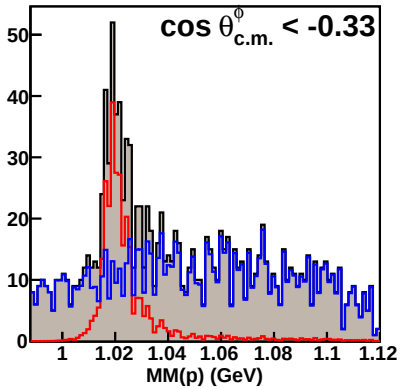

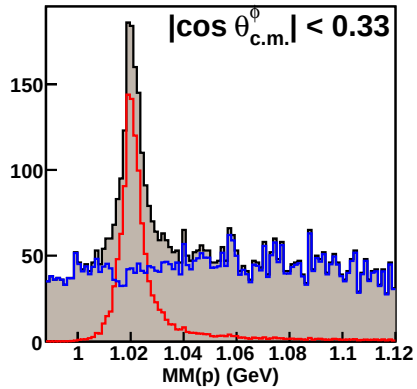

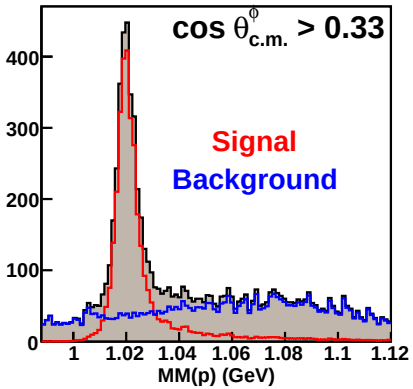

- $\sqrt{s} = 2.355$ GeV

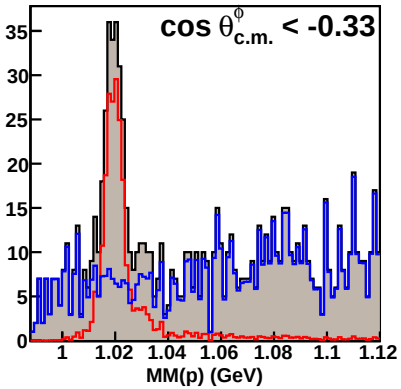

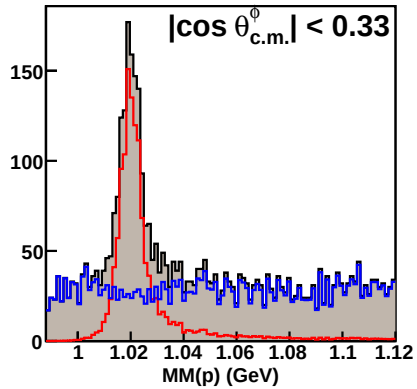

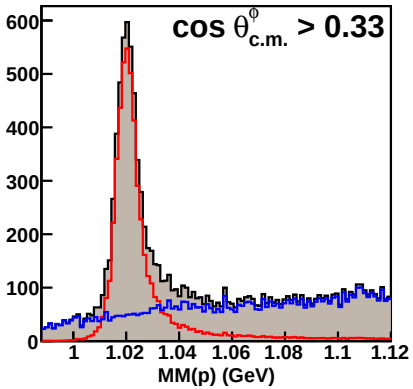

- $\sqrt{s} = 2.695$ GeV

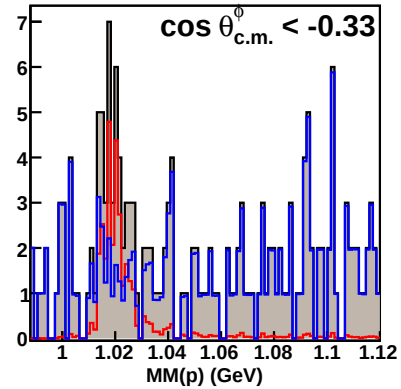

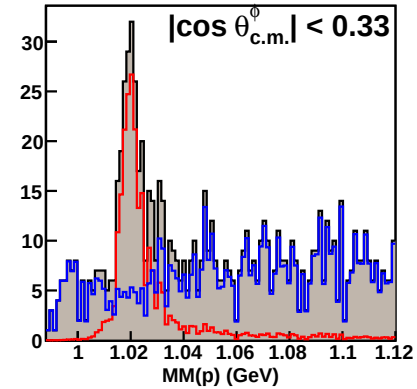

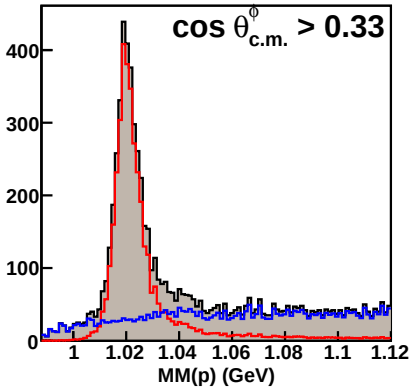

Neutral-mode: final results

- $\sqrt{s} = 2.105$ GeV

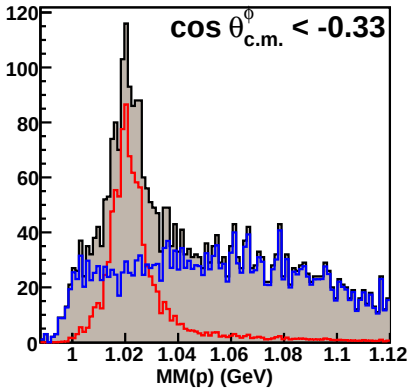

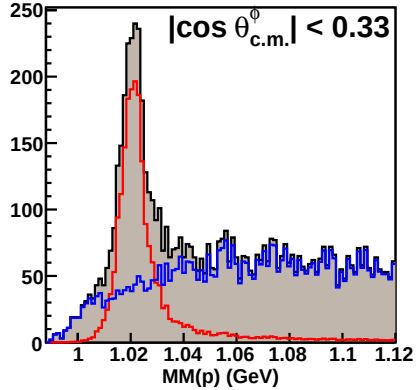

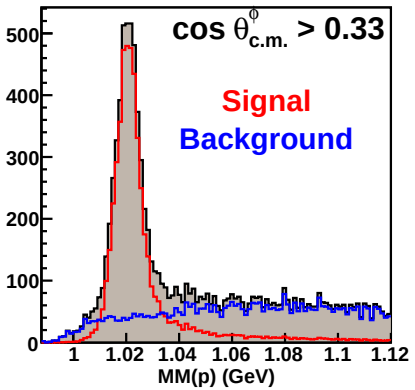

- $\sqrt{s} = 2.405$ GeV

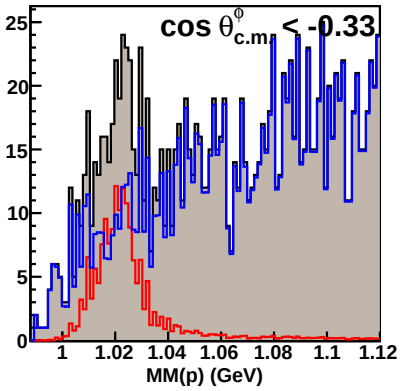

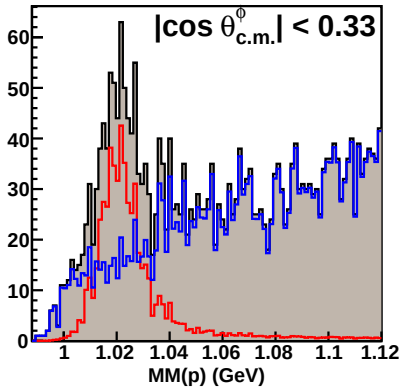

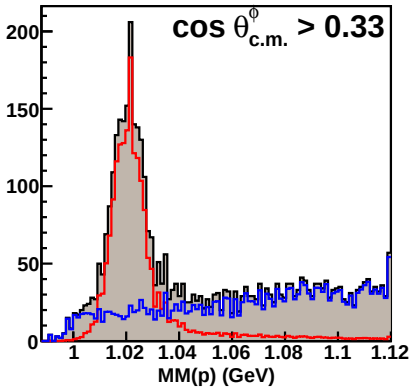

- $\sqrt{s} = 2.645$ GeV

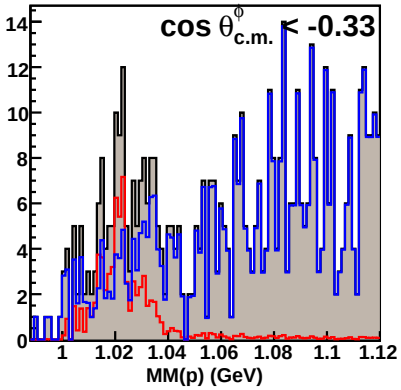

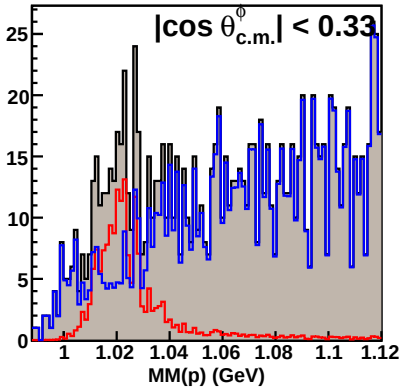

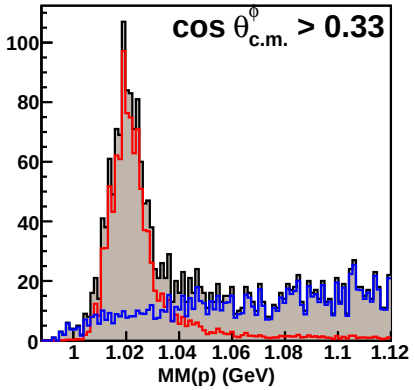

Final ϕ data yields and binning

- Charged-mode: ~ 0.475 million ϕ events. $\sqrt{s} = 10$-MeV-wide energy bins.
- Neutral-mode: ~ 0.101 million ϕ events. $\sqrt{s} \approx 30$-MeV-wide energy bins.
- Angular binning is always 0.1 in the center-of-mass production angle, $\cos\theta^{\phi}_{c.m.}$.

Outline

1. Introduction and Event Selection
2. Signal-background separation
3. Acceptance Calculation and $d\sigma/d\cos\theta^{\phi}_{c.m.}$
4. Spin Density Matrix Elements
5. Summary

Acceptance Calculation

- 100 million flat phase-space "Raw" Monte Carlo events generated for each topology and passed thru GSIM to give a set of "Accepted" (Acc) Monte Carlo events.
- Acc. MC underwent same set of analysis cuts as actual Data.
- Expand the scattering amplitude using a large number (almost complete basis) of s-channel J^P waves:

$$\mathcal{M}(\sqrt{s}, \cos\theta^{\phi}_{c.m.}) \sim \sum_{J^P} \alpha^{J^P}_{MP,LS} \mathcal{A}^{\gamma p \to J^P \to \phi p, MP, LS}_{m_\gamma, m_i, m_f, m_\phi}(\sqrt{s}, \cos\theta^{\phi}_{c.m.})$$

- Perform a unbinned extended maximum likelihood partial-wave analysis (PWA) fit independently in each $\sqrt{s}$-bin (see PRC 80, 065208 (2009) for more details).

Sample fit quality check

Charged-mode, center-of-mass production-angle:

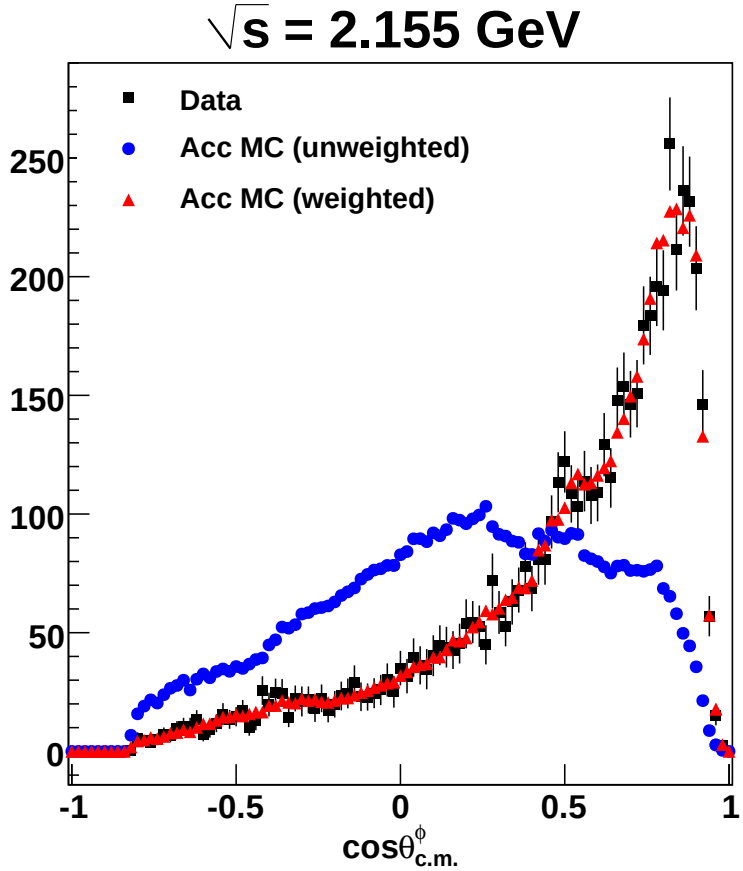

- PWA-fit weighted Monte Carlo matched the Data in all distributions for both modes.

Acceptance from PWA-fit results

- PWA-fit-weighted acceptance is: $\eta_{wtd.} = \left(\sum_i^{N_{acc}} I_i\right) / \left(\sum_j^{N_{raw}} I_j\right)$ where $I_i = \sum_{m_{incoh.}} |\sum_{m_{coh.}} \mathcal{M}_{m_{coh.},m_{incoh.}}|^2$.

- Note that this PWA-fit result is *not* to be interpreted as *physics* (in terms of resonances). We have simply expanded the production amplitude in a semi-complete basis of s-channel J^P waves in order to best fit the data.

- Applied in previous CLAS ωp (PRC 80, 06528 (2009)), $\eta p/\eta' p$ (PRC 80, 045213, (2009)), $K^+\Lambda$ (PRC 81, 025201 (2010)) and $K^+\Sigma^0$ (PRC 82, 025202 (2010)) analyses, with excellent results.

Differential cross sections

Backward-angles

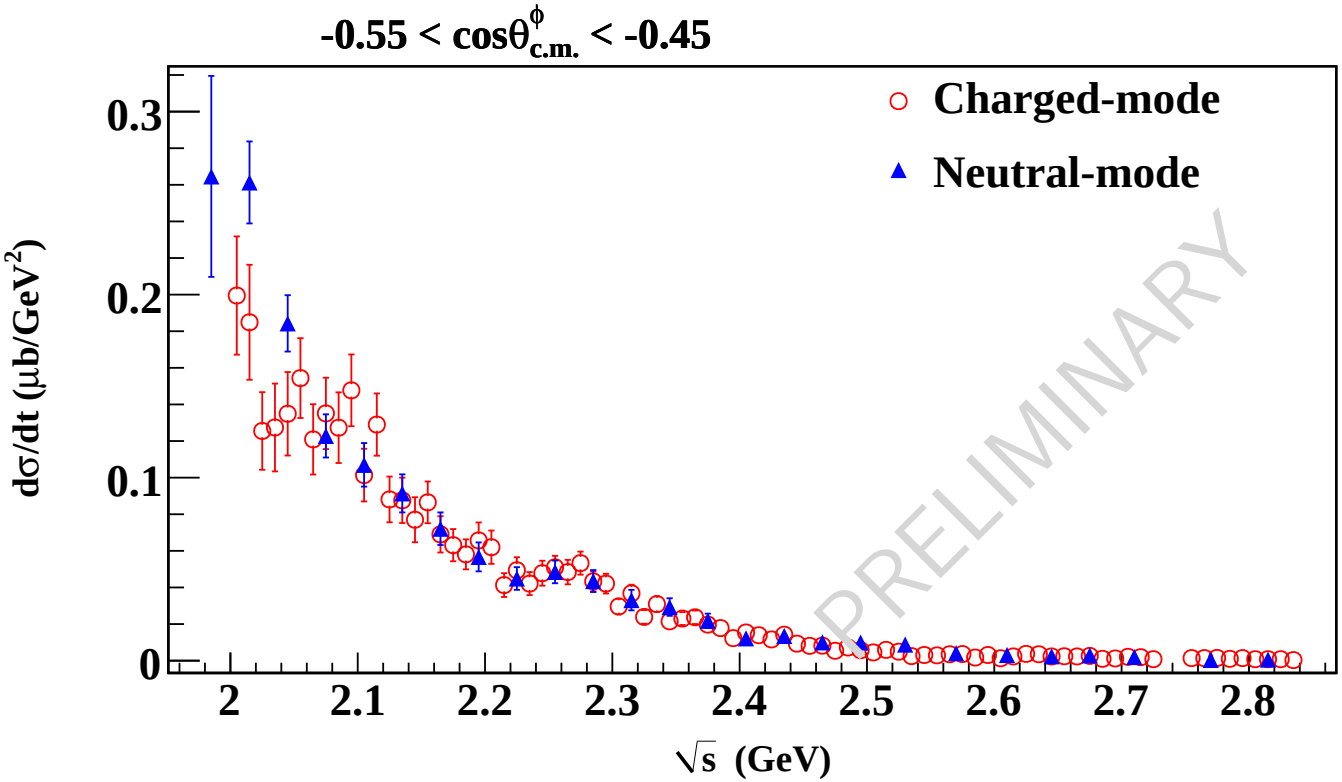

Differential cross sections

Mid-angles

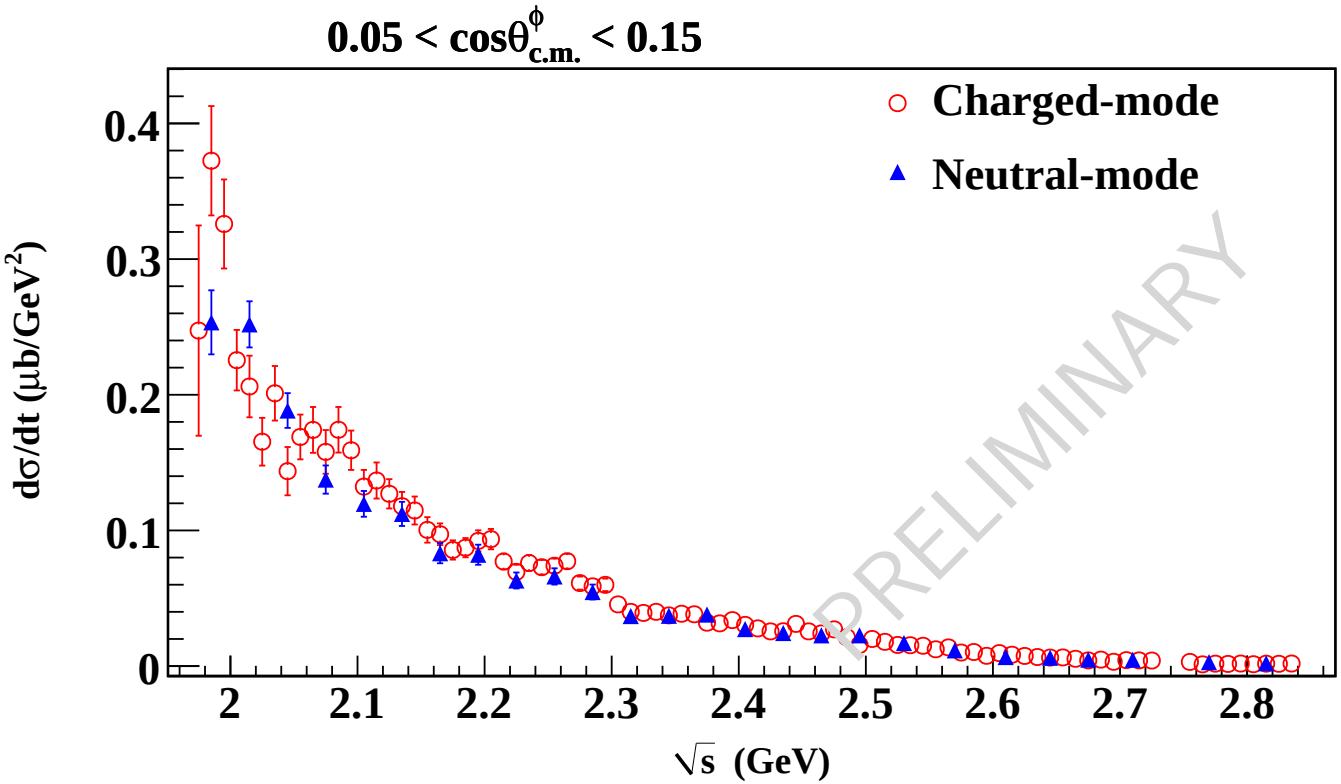

Differential cross sections

Forward-angles

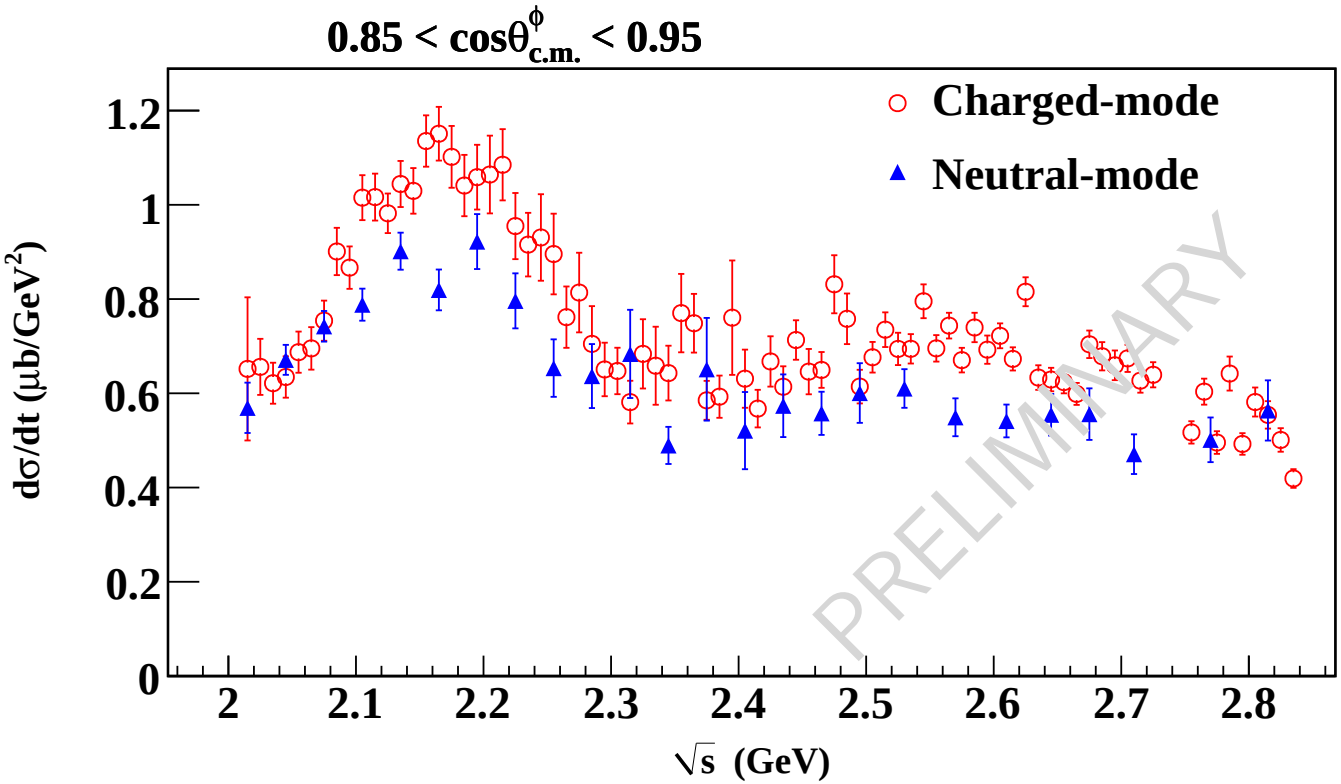

Comparison with SAPHIR '03 and LEPS '04

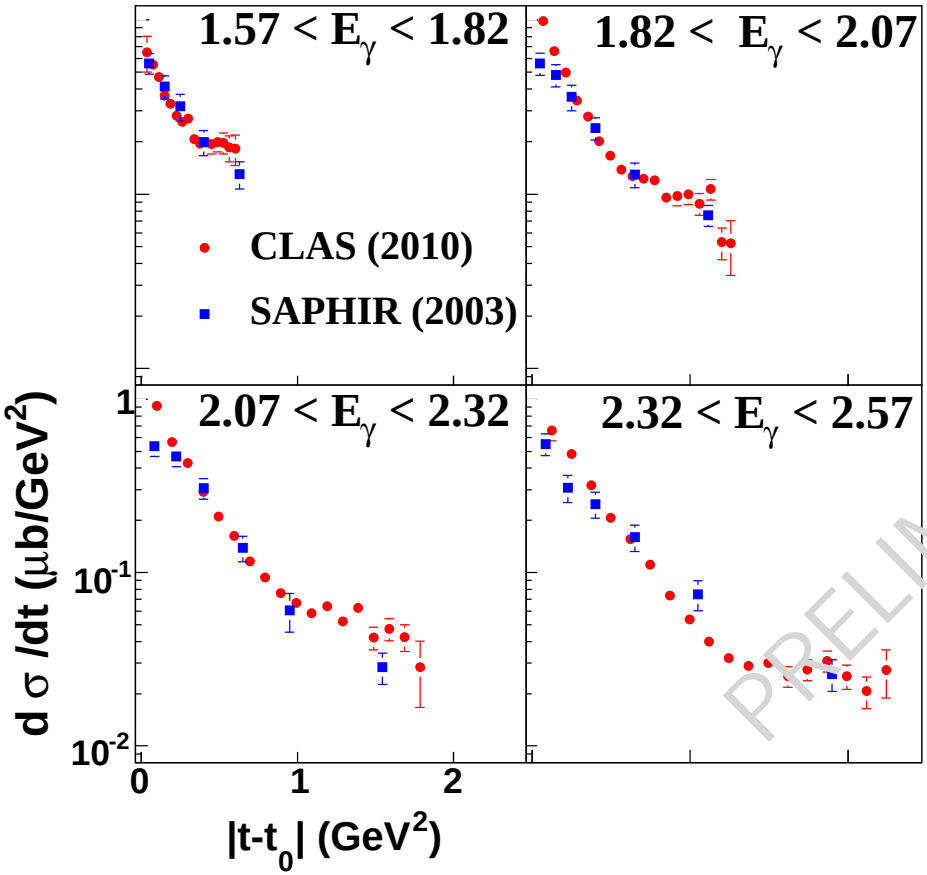

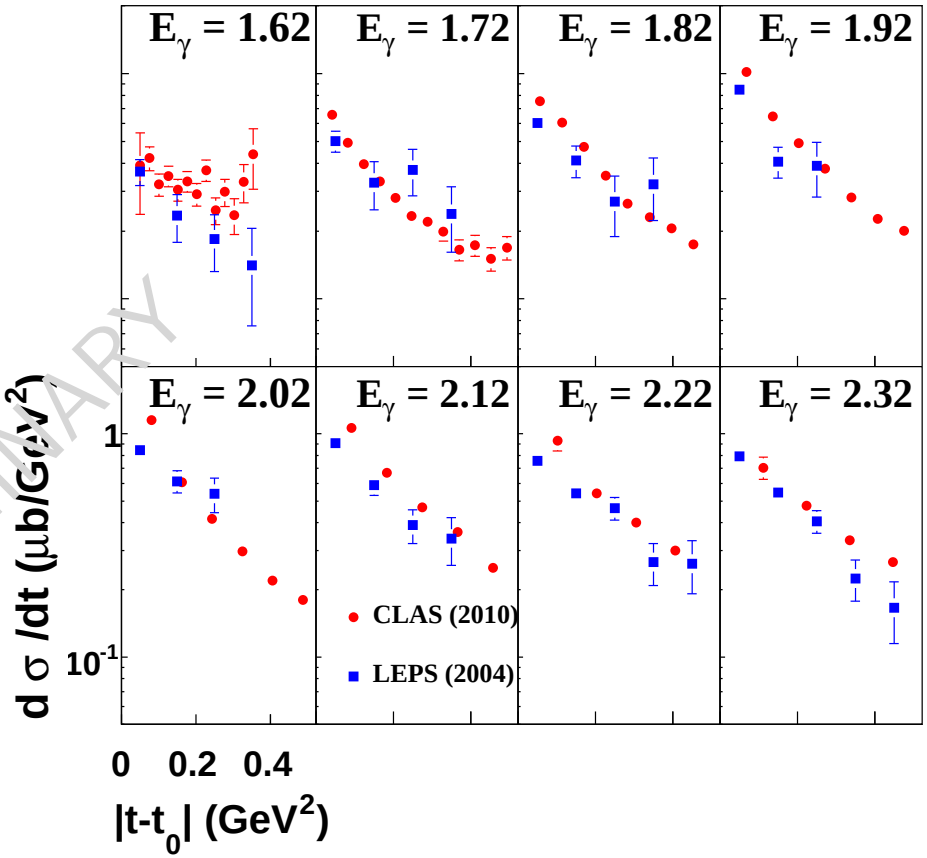

- Yield extraction is complicated since ϕ is so close to KK threshold. Physics model in MC could also make a difference, since forward-angle "bump" around $\sqrt{s} \sim 2.1$ GeV shows that simple diffractive Pomeron phenomenology is no longer valid.

Comparison with Daresbury '84 and CLAS '00

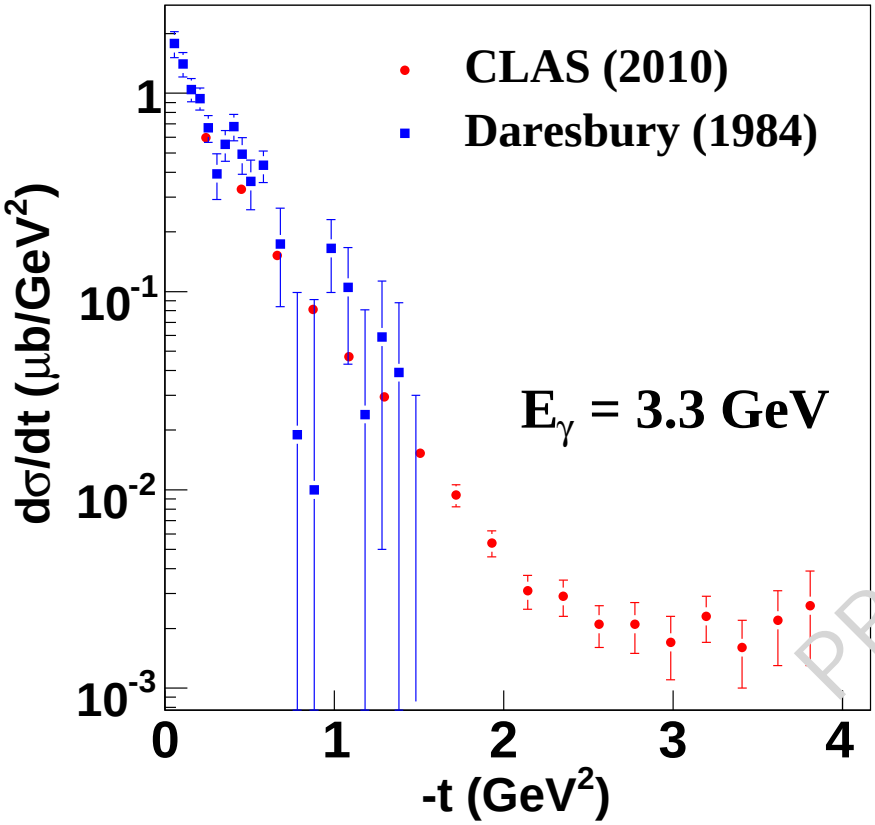

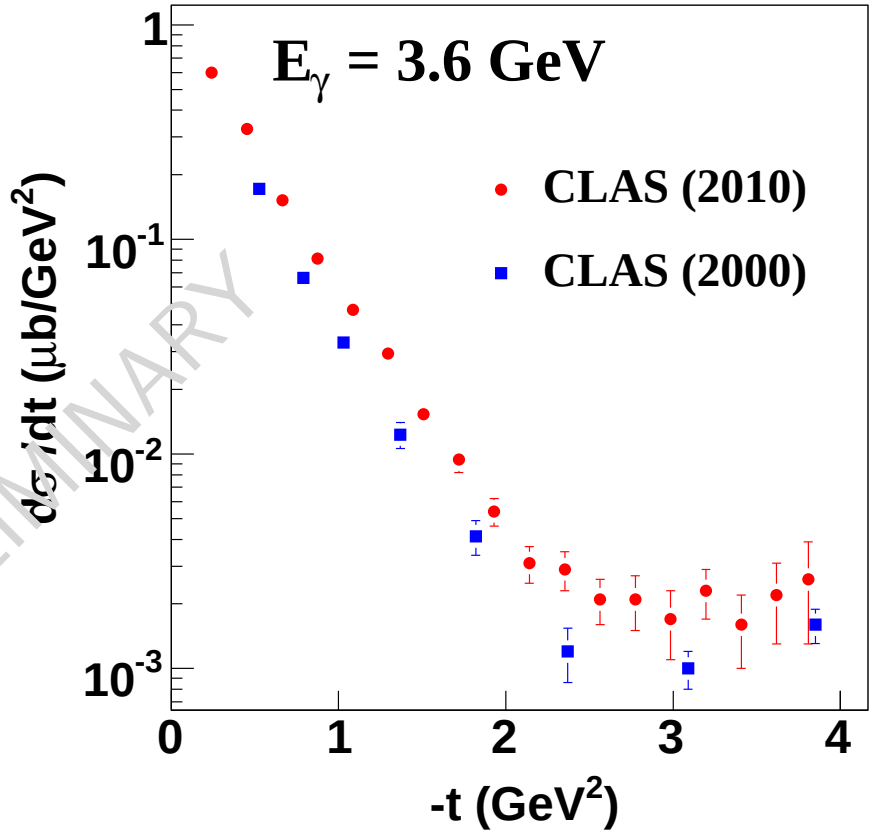

- E_γ bin-widths were 1 GeV (Daresbury-84) and 600 MeV (CLAS-00). Systematics of background subtraction/yield extraction in older ϕ results seem questionable.
- CLAS-2000 backward-angle rise confirmed by CLAS-2010: non-negligible $g_{\phi NN}$ for u-channel exchange at high $\sqrt{s}$.

Pomeron slope

- Fit to the form: $d\sigma/dt \propto \exp(-B_\phi|t - t_0|)$.

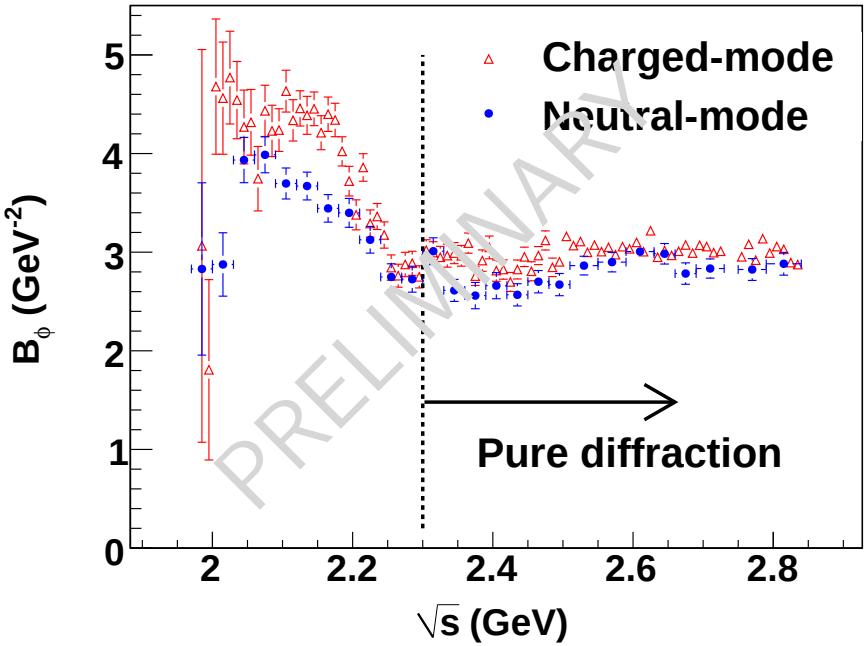

- Above $\sqrt{s} \sim 2.3$ GeV, in the purely diffractive regime, the Pomeron slope $B_\phi \approx 3$ GeV^{-2} and almost constant in this energy range.

- Below $\sqrt{s} \sim 2.2$ GeV, in the ϕ-$\Lambda(1520)$ overlap region, it is not a simple Pomeron phenomenology any longer.

The $\sqrt{s} \approx 2.1$ GeV "structure"

- Kiswandhi *et al.* (PLB 691, 214 (2010)): $3/2^-$ resonance around 2100 MeV.
- Ozaki *et al.* (PRC 80, 035201 (2009)): $K\Lambda(1520)$ and ϕp channels couple:

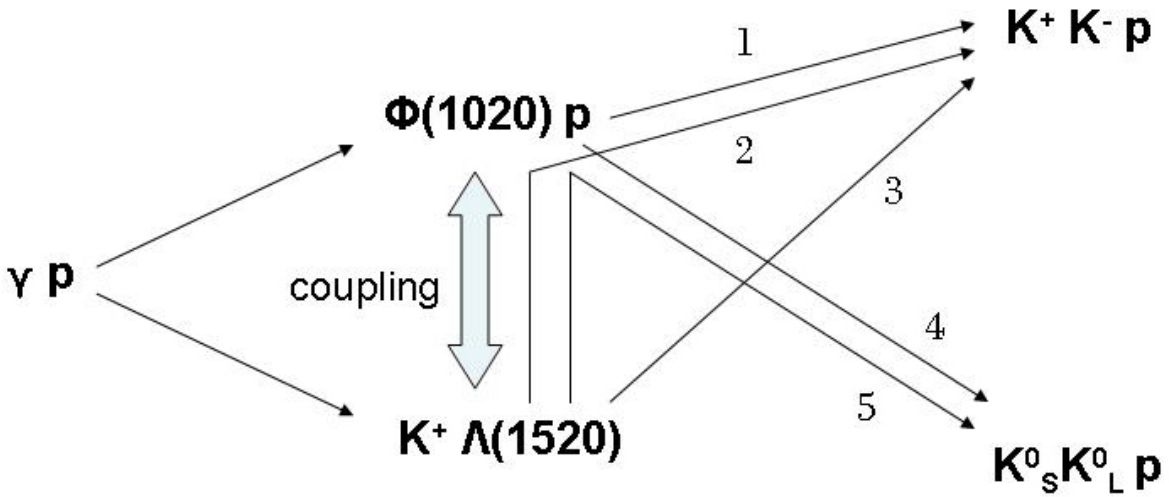

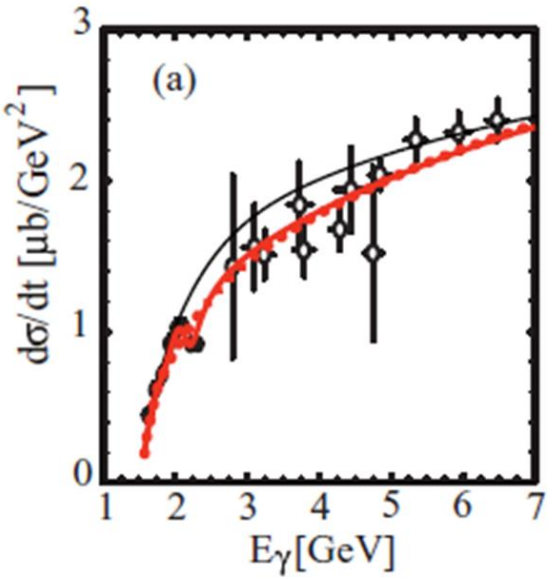

The $\sqrt{s} \approx 2.1$ GeV "structure" (contd.)

$\gamma p \to K^+\Lambda(1520)$:

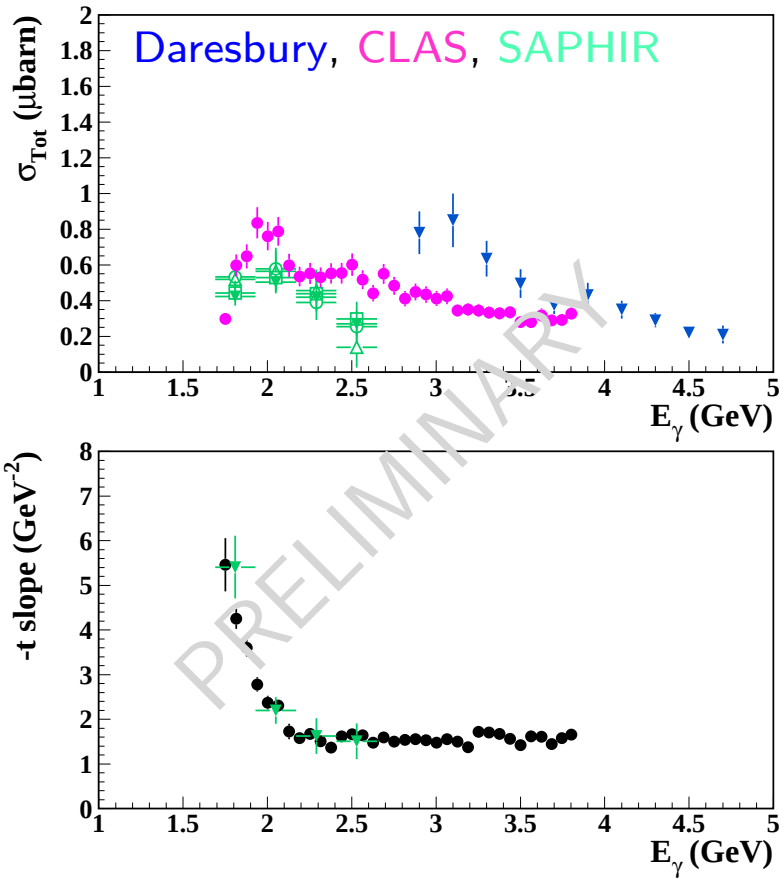

Work of R. De Vita *et al.*

- "Structures" also visible in $K^+\Lambda(1520)$ channel around $\sqrt{s} \sim 2.1$ GeV as well.
- Full ϕp-$K^+\Lambda(1520)$ coupled-channel analysis required to decipher the underlying physics.
- Also look at the $\Lambda(1520) \to \Sigma\pi$ mode, which doesn't share the same final states as ϕp charged-mode.

$R_{\phi/\omega}$ AND FLAVOR-INDEPENDENCE

Sibirtsev, *et al* PRD 71, 094011 (2005):

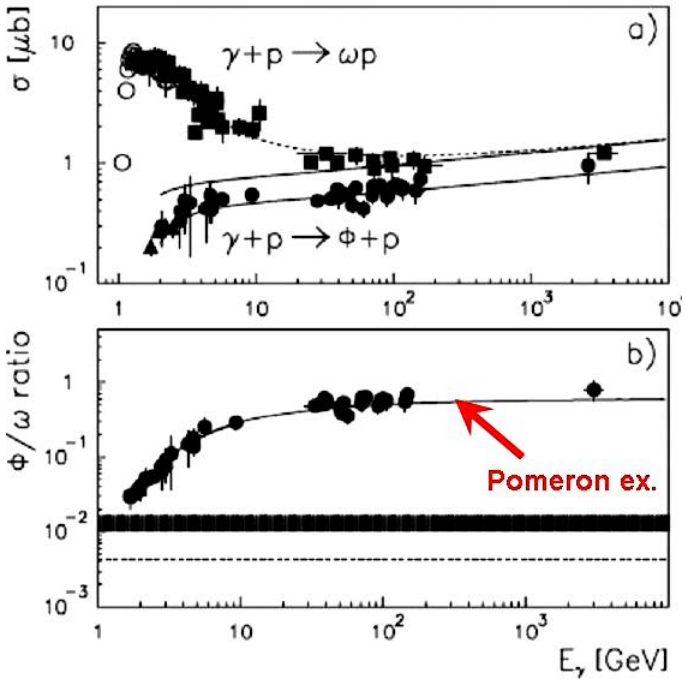

$R_{\phi/\omega}$ as a function of $(\cos\theta_{c.m.}, \sqrt{s})$:

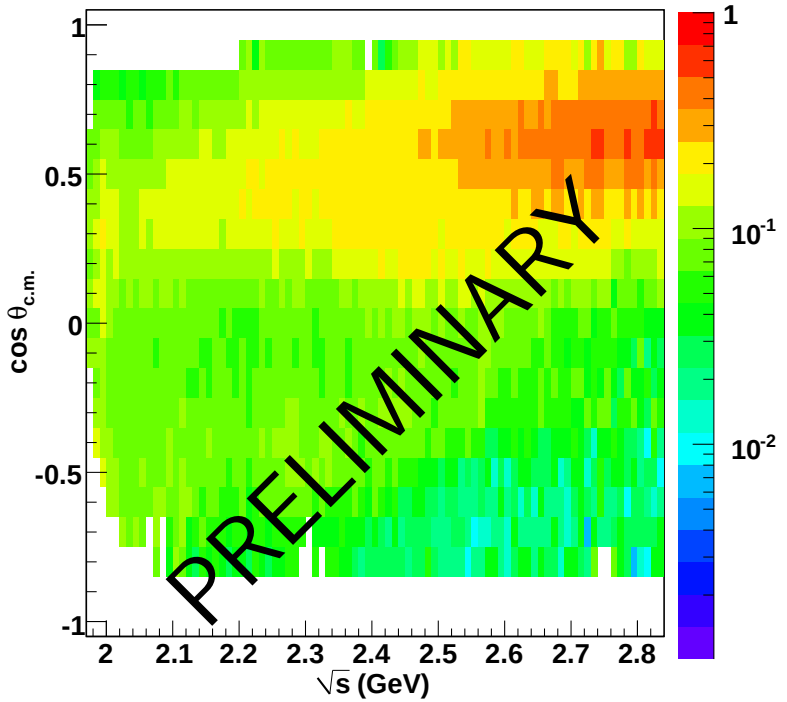

(CLAS ω: PRC 80, 065208 (2009))

- $R_{\phi/\omega}$ is generally small (OZI-suppression).
- In the diffractive limit where Pomeron dominates, $R_{\phi/\omega} \sim \mathcal{O}(1)$. Qualitatively agrees with Donnachie-Landshoff model: quark-quark-Pomeron coupling $\sim \beta_u \beta_s \bar{u}' \gamma_\mu u$. Couplings β almost flavor-independent.

Outline

1. Introduction and Event Selection
2. Signal-background separation
3. Acceptance Calculation and $d\sigma/d\cos\theta^{\phi}_{c.m.}$
4. Spin Density Matrix Elements
5. Summary

Spin Density Matrix Elements (SDME's)

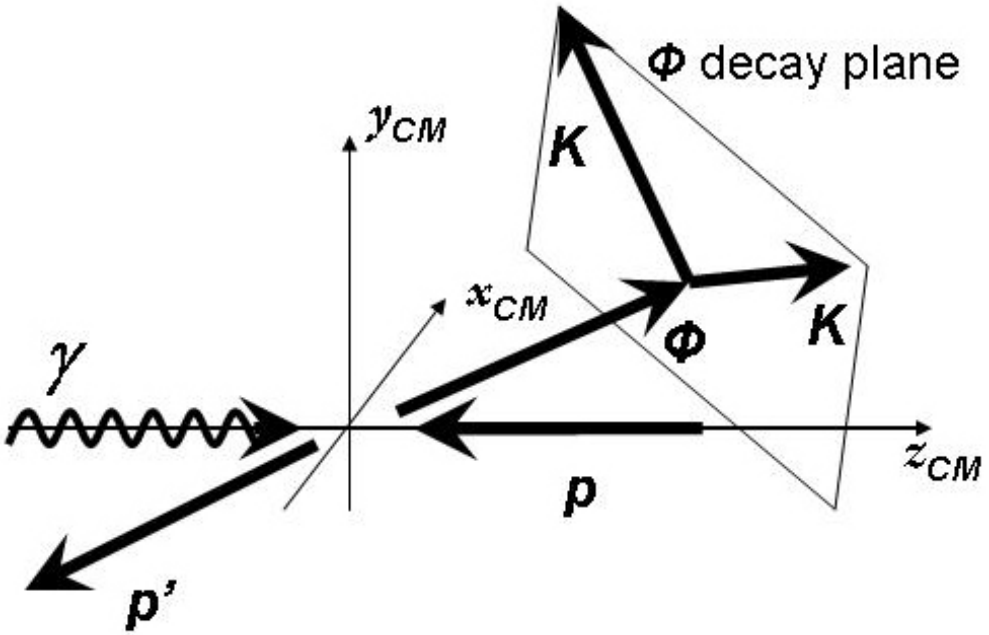

- With unpolarized beam and target, $\rho^0_{mm'}$ only accessible.
- Spin quantitation axis as the beam dirn. $\hat{z}_{CM}$ (Adair frame).
- ϕ rest frame decay angles: θ_{Ad} and φ_{Ad}.

- Conventional Schilling's method: fit to an $\phi \longrightarrow KK$ decay angular intensity distribution:

$$\mathcal{I}(\sqrt{s}, \cos\theta^{\phi}_{c.m.}) \sim \tfrac{1}{2}(1-\rho^0_{00}) + \tfrac{1}{2}(3\rho^0_{00}-1)\cos^2\theta_{Ad} - \rho^0_{1-1}\sin^2\theta_{Ad}\cos 2\varphi_{Ad} - \sqrt{2}Re\rho^0_{10} sin2\theta_{Ad}\cos\varphi_{Ad}$$

- Equivalently, direct construction of the ϕ density matrix using PWA fit results:

$$\rho^0_{mm'} = \frac{\sum \mathcal{A}^m \mathcal{A}^{m'*}}{\sum |\mathcal{A}^m|^2 + |\mathcal{A}^{m'}|^2},$$

where m, m' are ϕ spin-projections and incoherent sum is over the spins of γ, p, and p'.

SDME RESULTS (CHARGED-MODE)

Adair frame:

Backward-angles

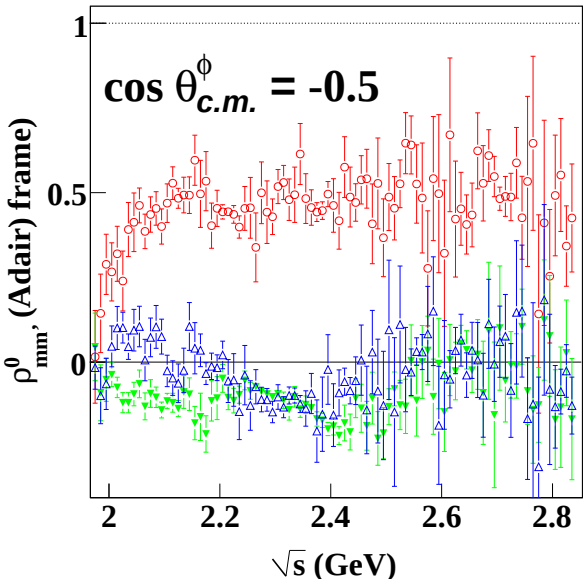

Mid-angles

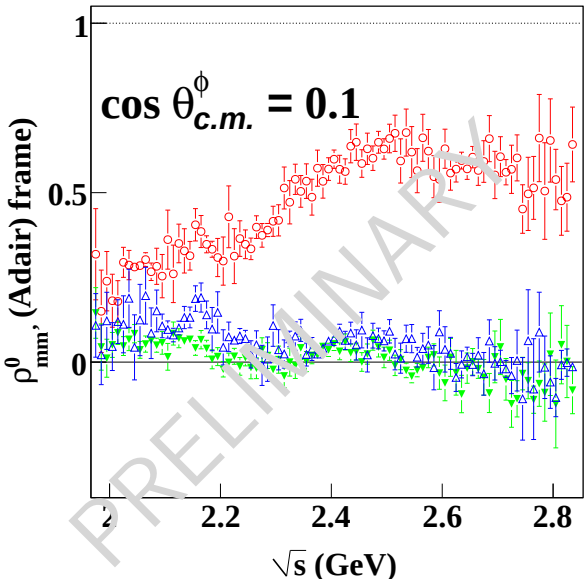

Forward-angles

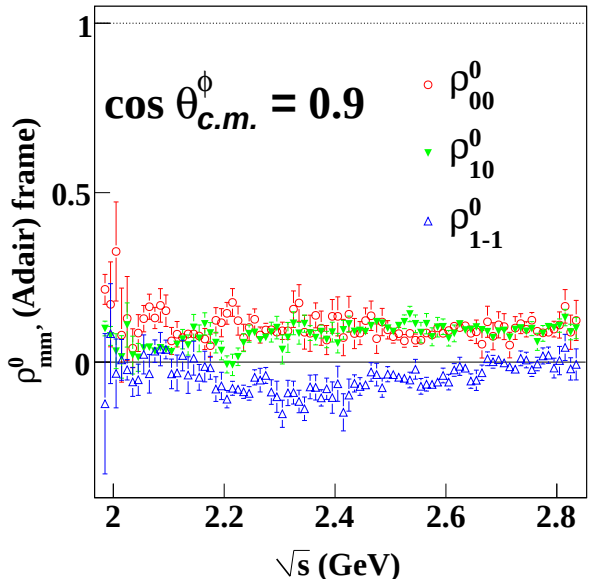

- $\sqrt{s}$ = 10-MeV-wide energy bins.

SDME: COMPARISON BETWEEN ϕ AND ω RESULTS

- Adair frame ρ^0_{00}: "hump" followed by a "dip" for both channels.
- Position of the "dip" in $\cos\theta_{c.m.}$ is different for the two vector mesons.

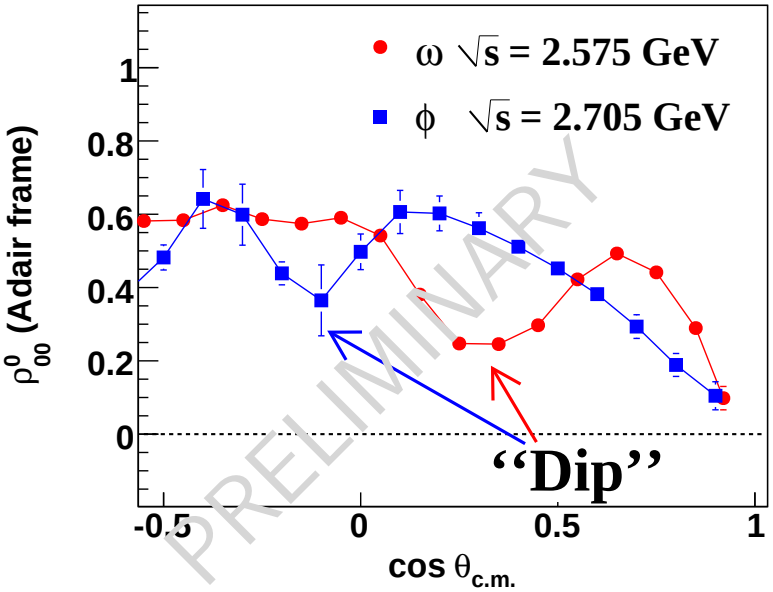

SDME: COMPARISON BETWEEN ϕ AND ω RESULTS

- Adair frame ρ^0_{00}: "hump" followed by a "dip" for both channels.
- Position of the "dip" in $\cos\theta_{c.m.}$ is different for the two vector mesons.
- Present theory models don't describe this dip very well – shown on the right for the ω case. Room for improvement.

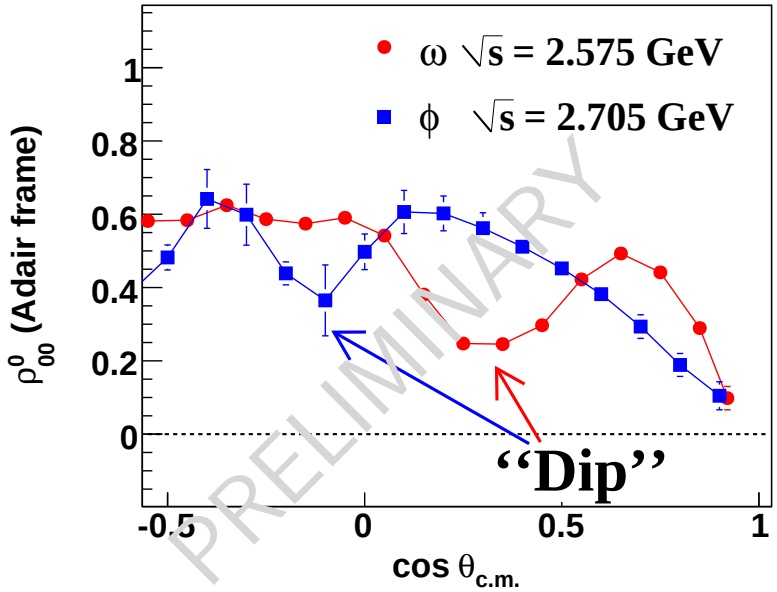

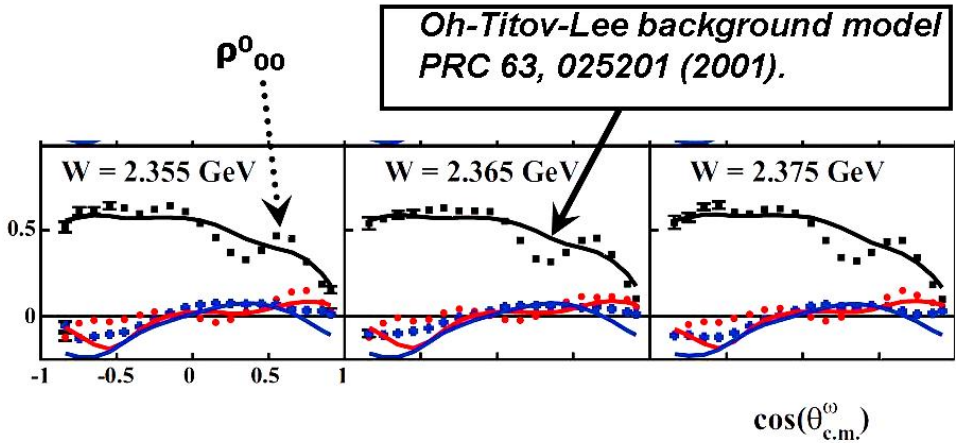

CLAS ω PWA, Williams et al. (PRC 60, 065209 (2009))

SCHC VIOLATION

- Naively, Pomeron (0^{++} exchange) should conserve t-channel helicity (TCHC). Instead, experimentally, TCHC is broken and s-channel helicity is seen to be conserved (SCHC).

- Phenomenological explanation by Gilman *et al.* (PLB 31, 387 (1970)). However, no *fundamental* reason for SCHC.

- New CLAS results show $\rho^0_{00} \neq 0$: both TCHC and SCHC violation at all angles (both ϕ and ω channels, in fact).

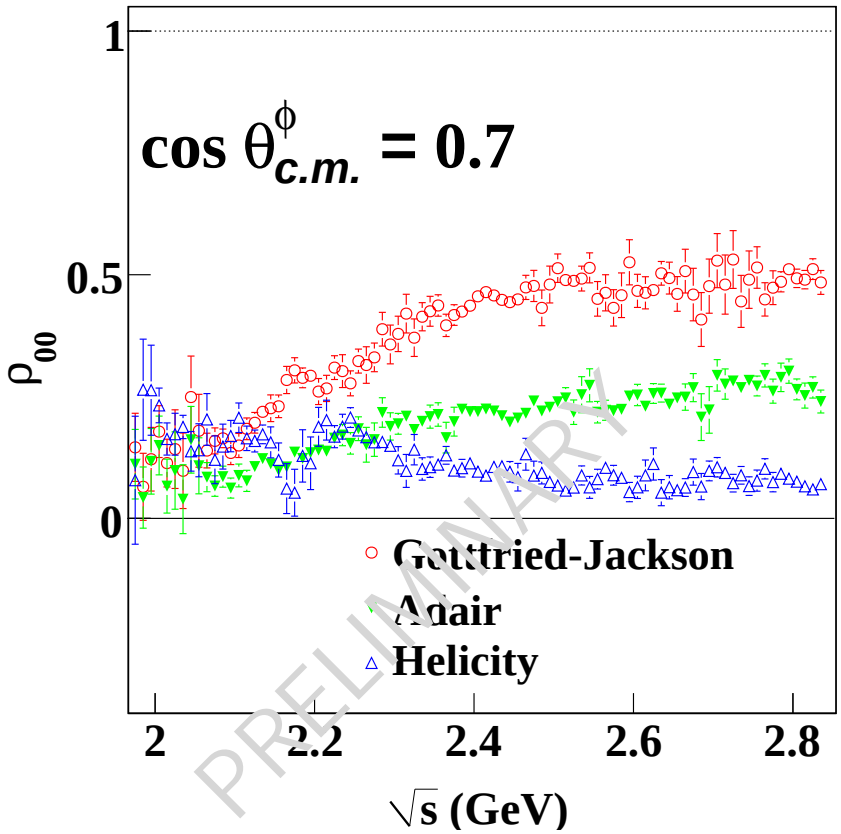

Comparison with LEPS (charged-mode)

- Previous SDME measurements: *highly* statistics limited, wide energy bins.
- Often averaged over angular variables in Schilling's intensity expression, without proper acceptance correction.
- Latest forward-angle LEPS results (Chang PRC 82, 015205 (2010)) incorporates several improvements and are in overall good agreement with us.

Gottfried-Jackson frame:

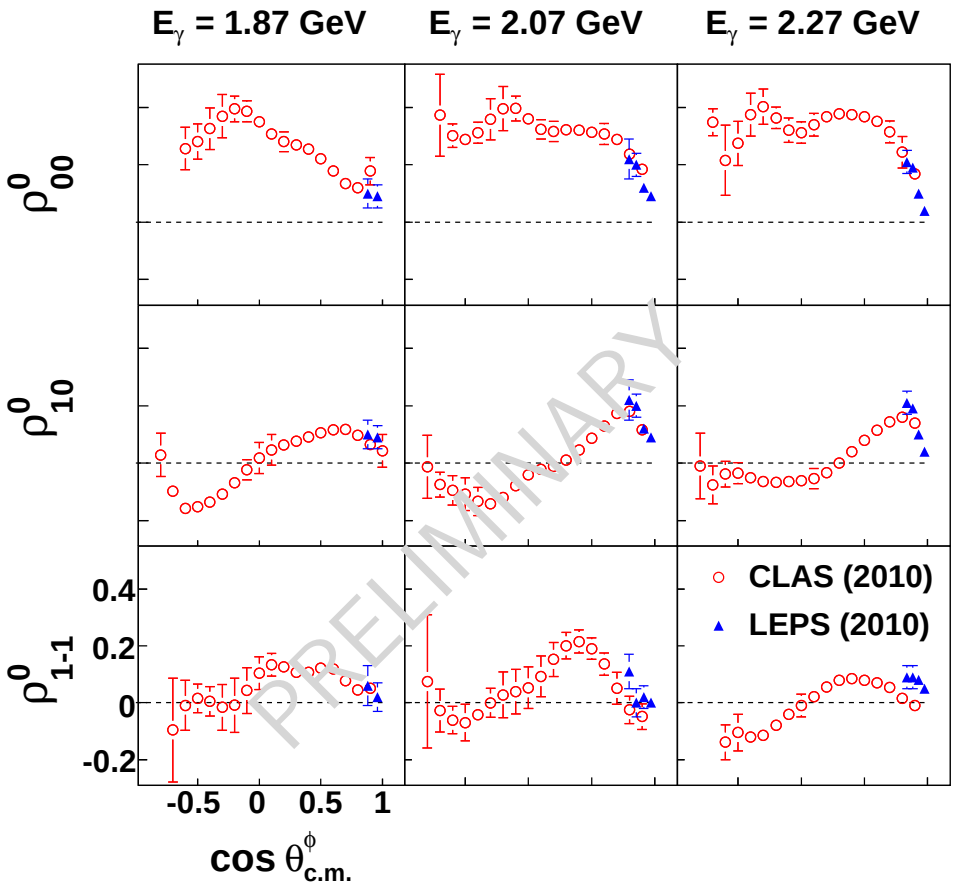

SDME Charged- and neutral-mode comparison

- Neutral-mode SDME's also extracted in exactly similar way as for the charged-mode.
- Some local differences visible around $\sqrt{s} \sim 2.1$ GeV region.
- Further studies to be done on the charged-mode "structures" before finalizing results.

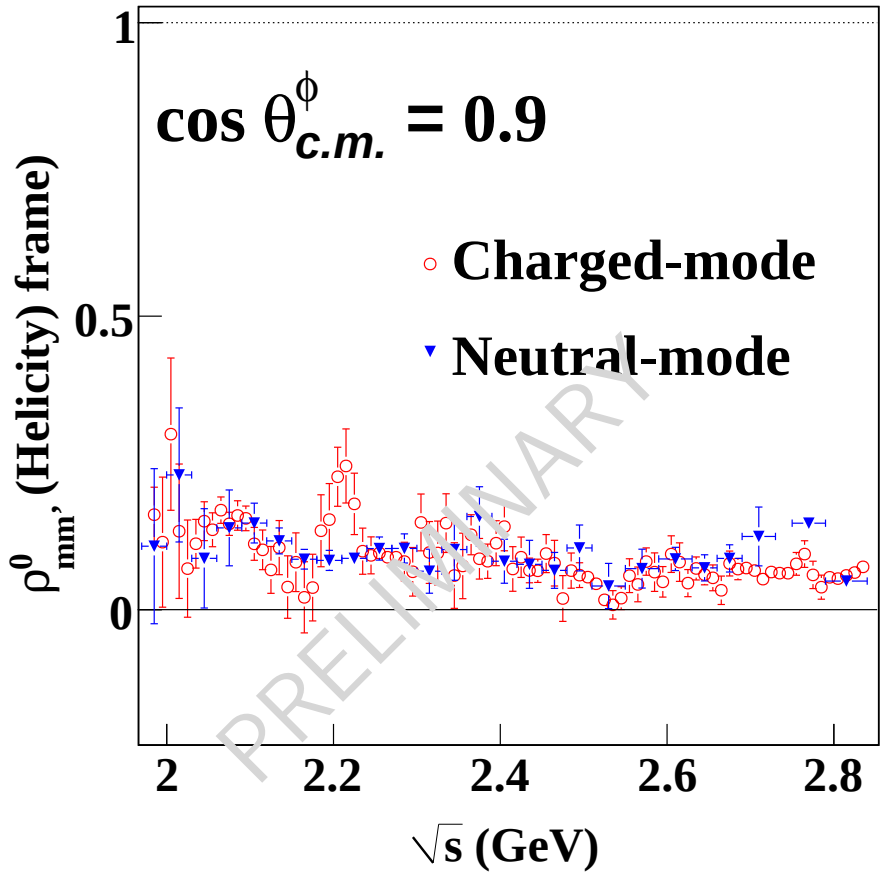

Outline

1. Introduction and Event Selection
2. Signal-background separation
3. Acceptance Calculation and $d\sigma/d\cos\theta^{\phi}_{c.m.}$
4. Spin Density Matrix Elements
5. Summary

Summary

- First ever extensive world data for the ϕ channel. Corresponding ω results already published by the CLAS Collaboration.
- Detailed $d\sigma/dt$ and $\rho^0_{mm'}$: coverage from near threshold to $\sqrt{s} = 2.84$ GeV and $-0.85 \leq \cos\theta^{\phi}_{c.m.} \leq 0.95$.
- Access to both charged- and neutral-modes results is a very useful tool.
- "Structure" around $\sqrt{s} \sim 2.1$ GeV needs careful study. Present results will provide detailed information towards this.
- *Lots* of interesting features visible in the new data – SCHC violation, finite value of $g_{\phi NN}$, Pomeron slope etc.
- Full partial-wave analysis on both ϕ and ω currently underway. CLAS $\Lambda(1520)$ results from the same dataset soon to be available as well for coupled-channel analysis.

Event-selection: timing cuts

- 2-D calculated mass cut on p, K^+ (charged-mode)

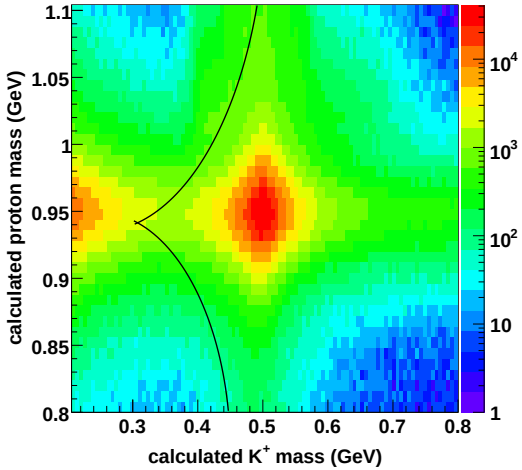

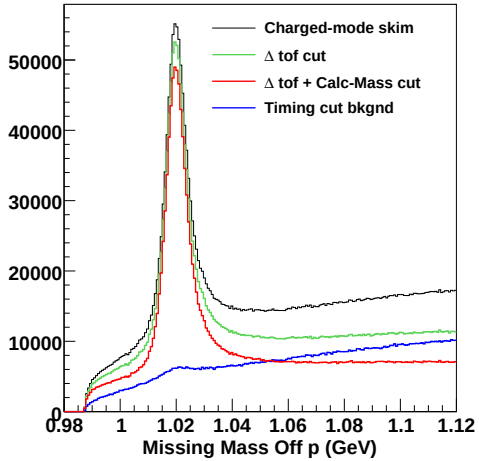

accepted
rejected

- 2-D Δtime-of-flight ($tof_{meas} - tof_{calc}$) cut on p, π^+ (neutral-mode)

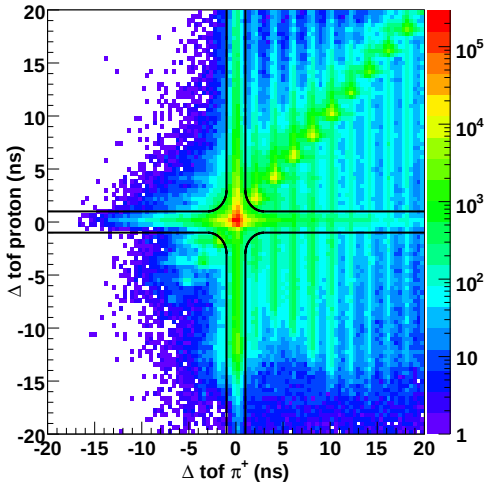

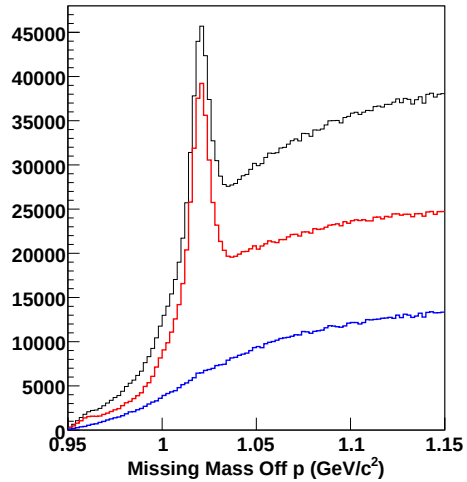

Event-selection contd.

- K^0_S selection cut (neutral-mode): $0.488\ \text{GeV} \leq M(\pi^+, \pi^-) \leq 0.508\ \text{GeV}$.

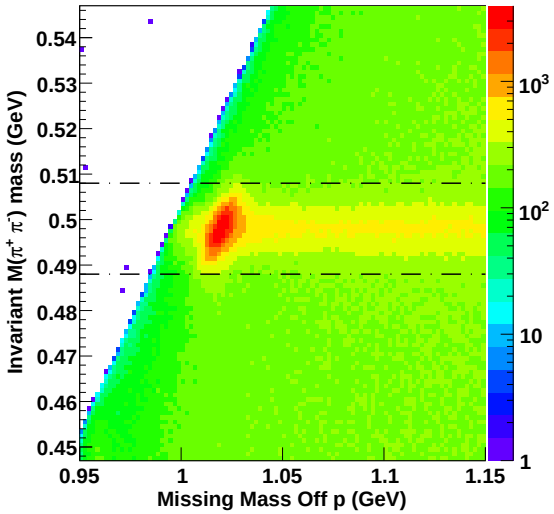

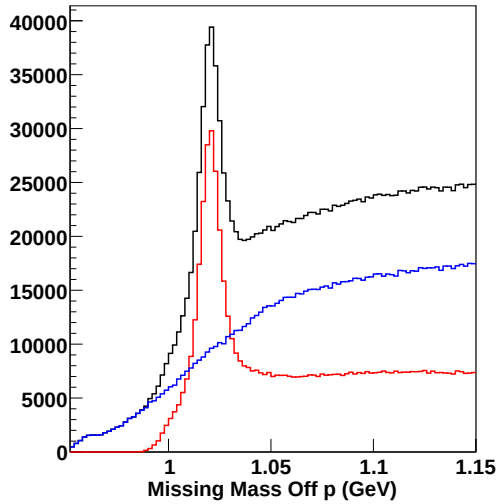

accepted, rejected

ϕ LINESHAPE

- ϕ width is $\Gamma_0 \approx 4$ MeV, however, its mass being so close to the KK threshold (≈ 0.99 GeV) leads to a unsymmetric lineshape.
- All previous world data relied on a Gaussian ϕ lineshape for yield extraction fits.
- We've tried to employ a better approximation by taking a mass-dependent width:

$$\Gamma(m) = \Gamma_0 \left(\frac{q}{q_0}\right)^{2L+1} \left(\frac{m_0}{m}\right) \left(\frac{B_0}{B}\right)$$

- $L = 1$ for P-wave $\phi \to KK$ decay.
- Break-up momentum $q(m) = \sqrt{m^2 - m_K^2}/2$ for a ϕ mass m.
- Barrier-factor $B_{L=1} = \sqrt{2z/(1+z)}$ with $z = q/d$, $d \sim 1$ fm (≈ 0.1973 GeV).
- Subscript 0 denotes evaluation at the ϕ mean mass $m_0 = 1.01946$ GeV.
- Final signal-function in background fits: Voigtian with Breit-Wigner width taken as $\Gamma(m)$.

LEPS BACKGROUND SEPARATION

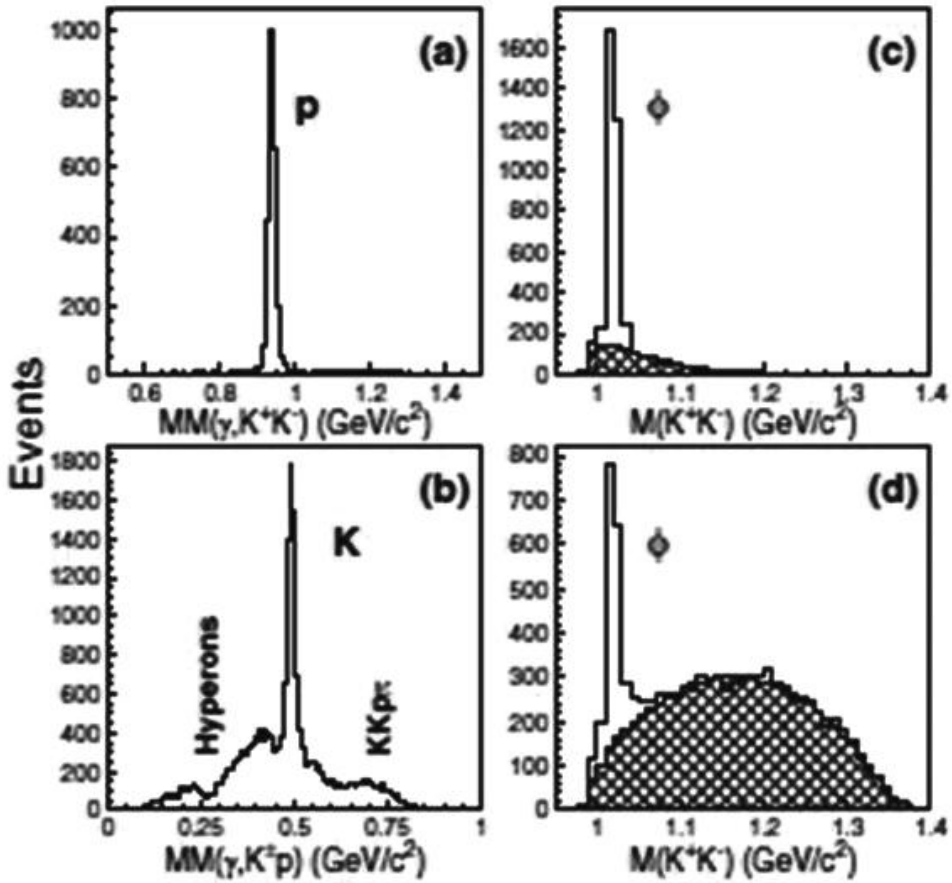

FIG. 1. (a) Missing mass distribution for the $p(\gamma, K^+K^-)X$ reaction in KK mode. (b) Missing mass distribution for the $p(\gamma, K^{\pm}p)X$ reaction in Kp mode. (c) and (d) are the K^+K^- invariant mass distributions after the cut on the missing mass for KK and Kp modes, respectively. The hatched histograms are the simulated background.

SAPHIR background separation

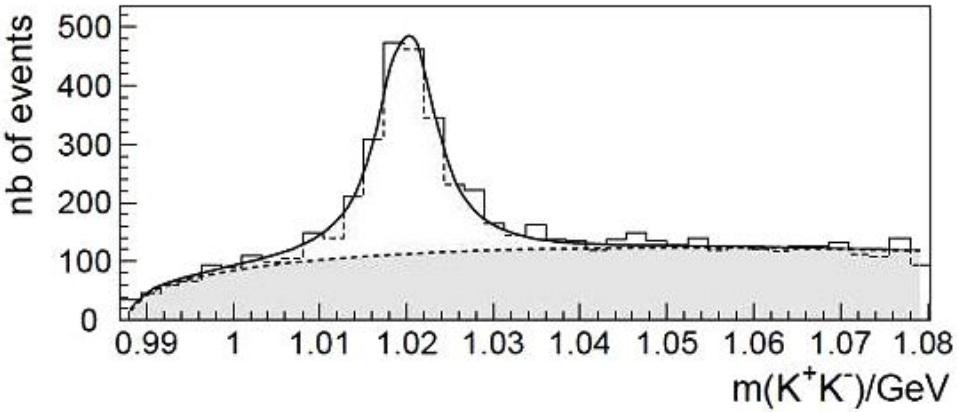

Fig. 3. Φ separation from the background in the K^+K^- mass spectrum.

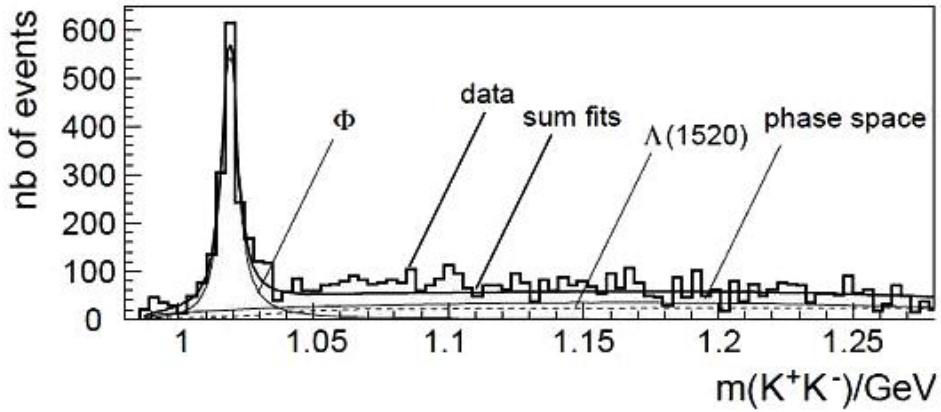

Fig. 4. Contributions of phase space, Λ(1520) and Φ production to the K^+K^- mass spectrum for photon energies between 2.1 and 2.4 GeV.

Anciant background separation

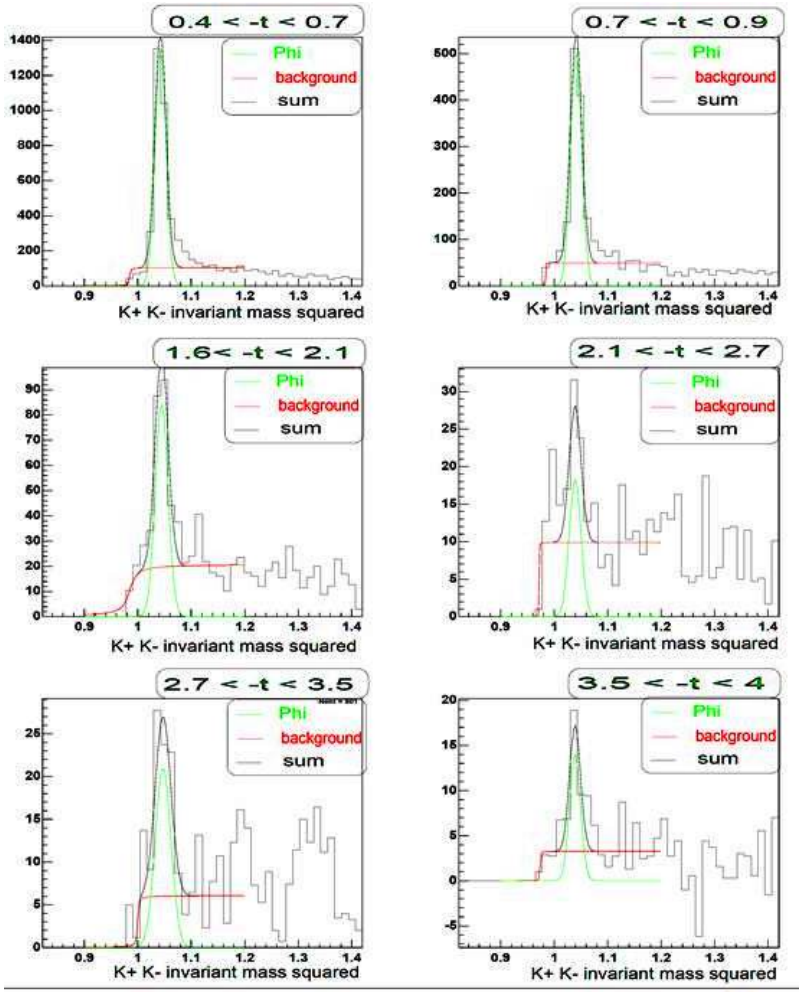

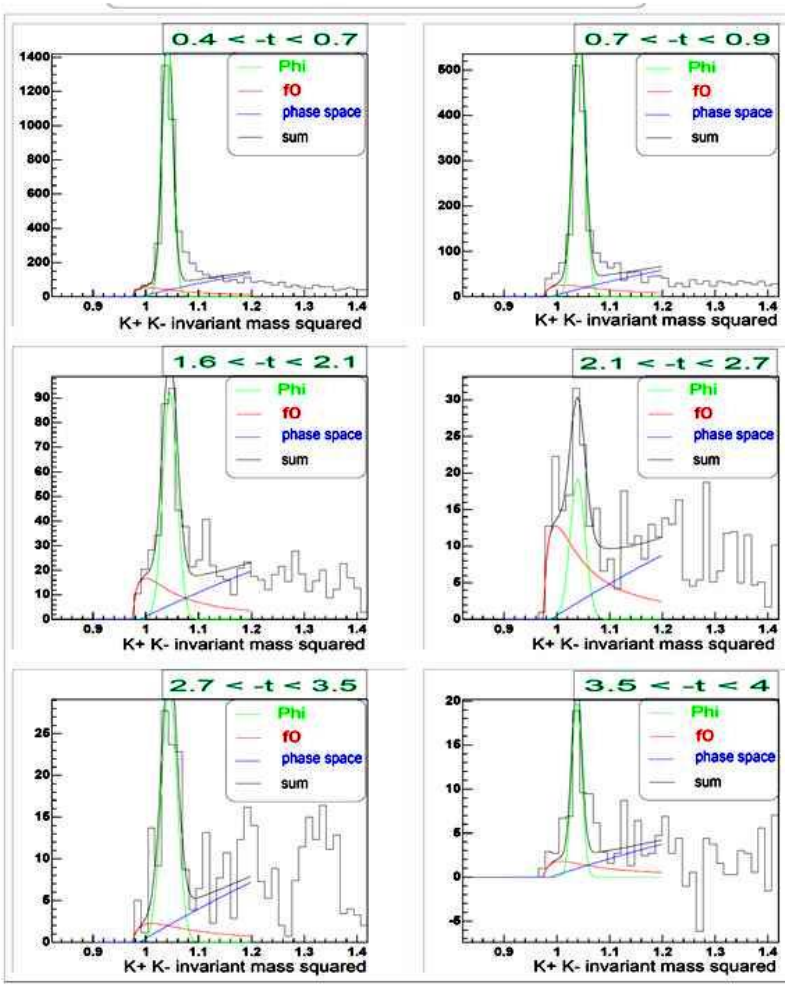

Fit quality checks

Charged-mode

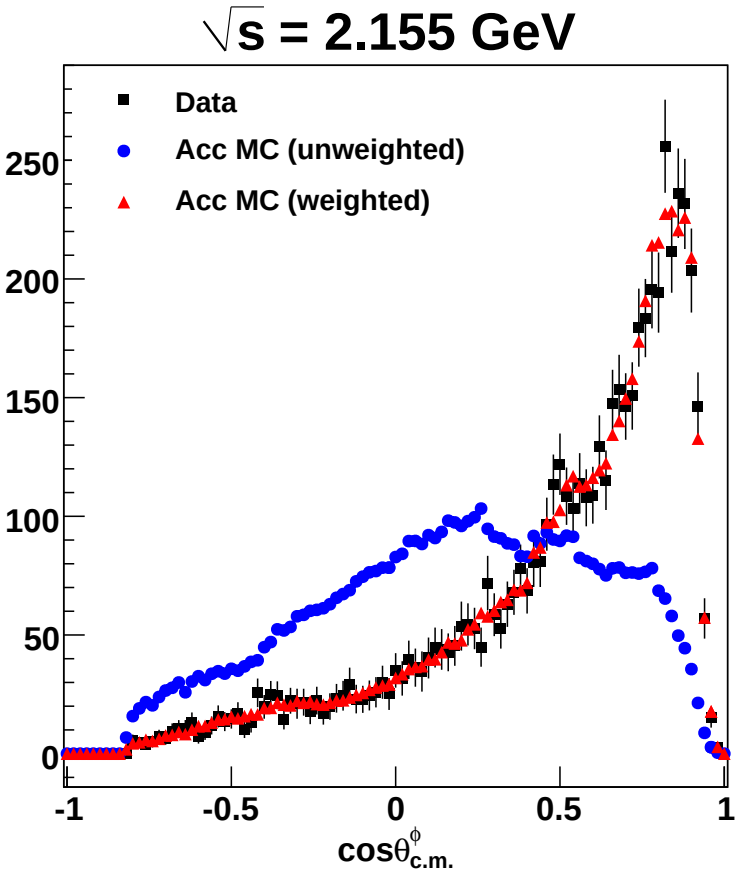

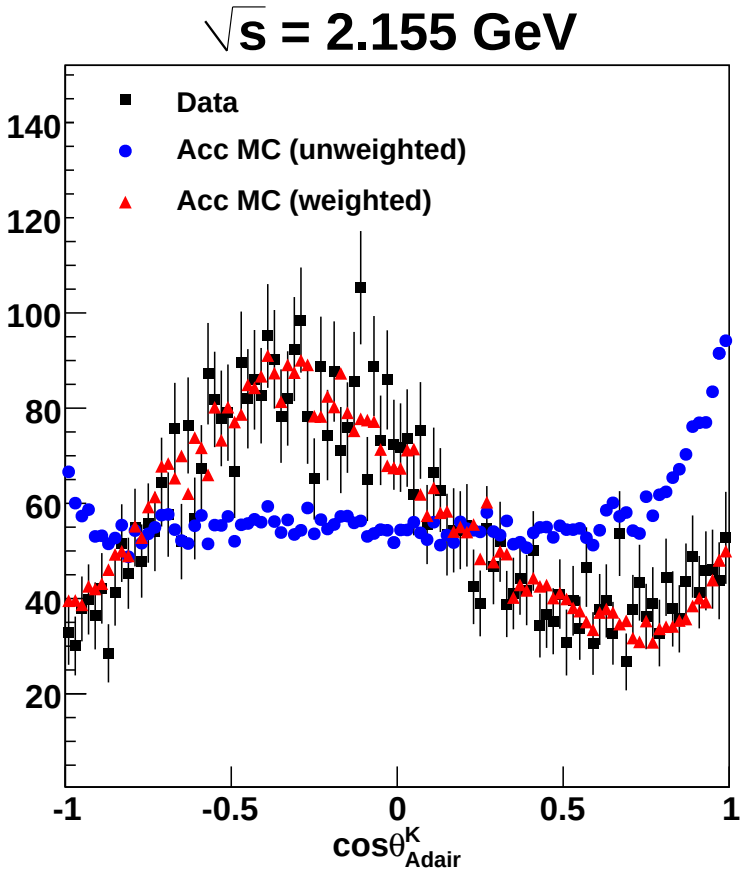

Fit quality checks (contd.)

Neutral-mode

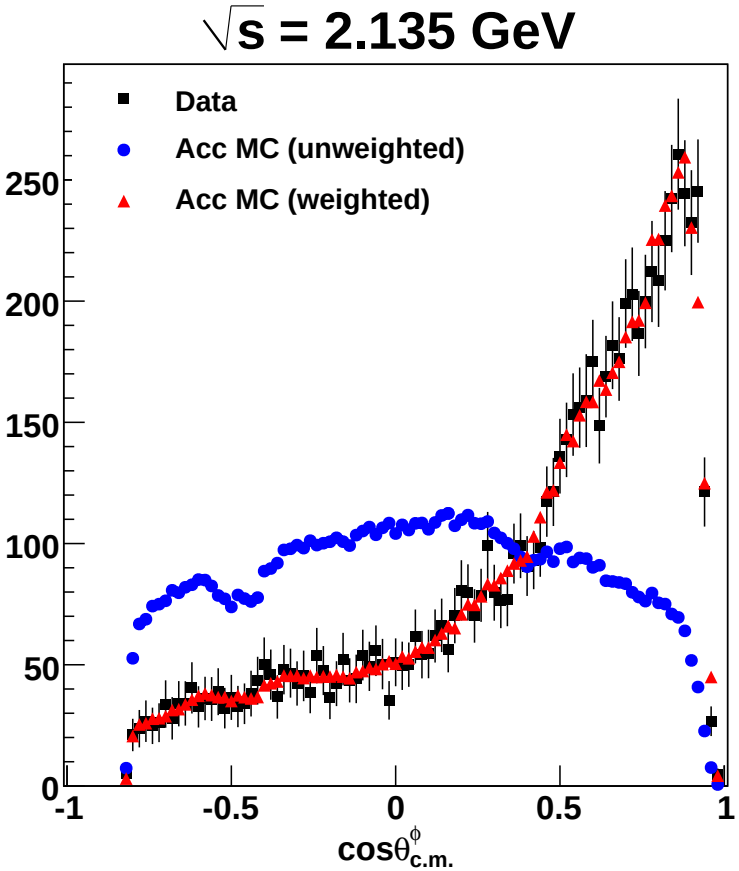

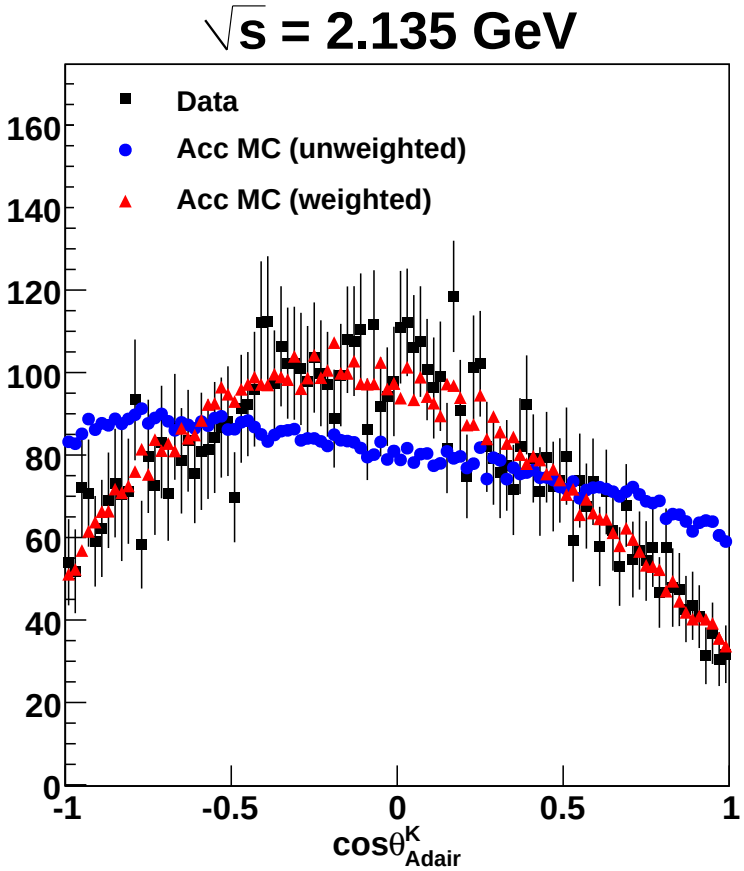
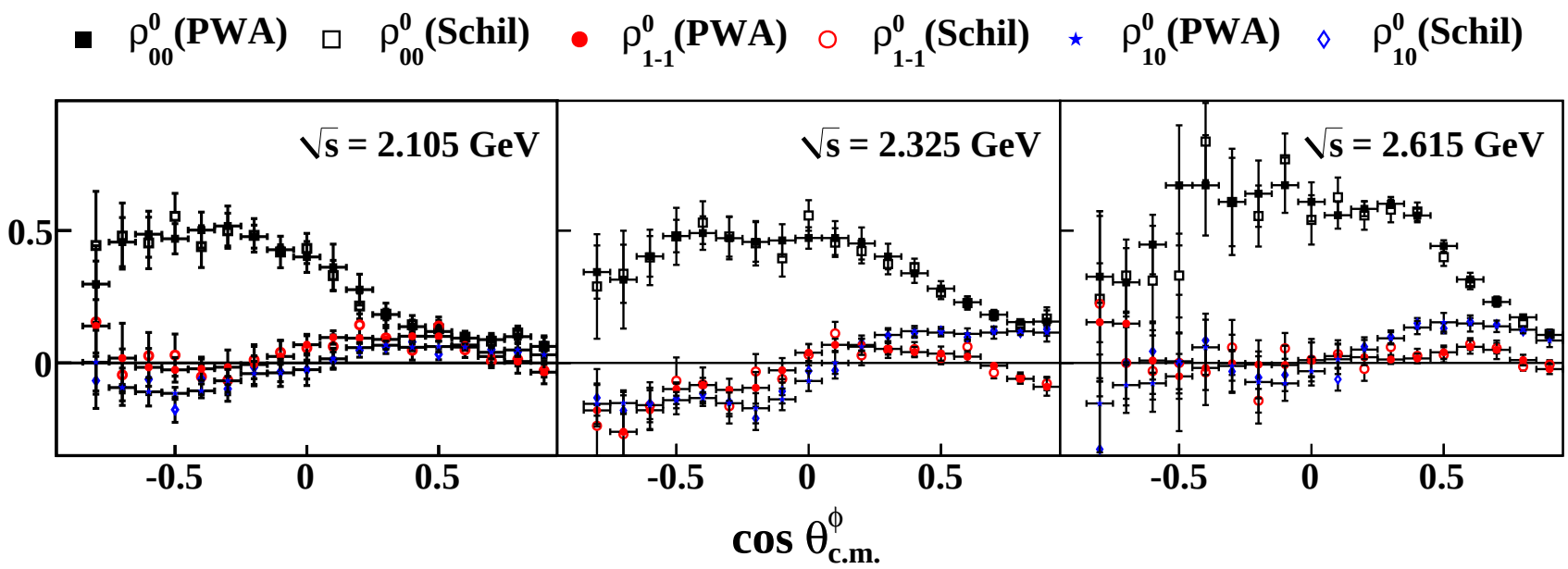
Comparison between PWA and Schilling's methods